

EFFECT OF DOUBLE LAYERS ON MAGNETOSPHERE-IONOSPHERE COUPLING

Robert L. Lysak
School of Physics and Astronomy, University of Minnesota
Minneapolis, MN 55455, U.S.A.

N87-23321

Mary K. Hudson
Department of Physics and Astronomy, Dartmouth College
Hanover, NH 03755, U.S.A.

ABSTRACT

The Earth's auroral zone contains dynamic processes occurring on scales from the length of an auroral zone field line (about $10 R_E$) which characterizes Alfvén wave propagation to the scale of microscopic processes which occur over a few Debye lengths (less than 1 km). These processes interact in a time-dependent fashion since the current carried by the Alfvén waves can excite microscopic turbulence which can in turn provide dissipation of the Alfvén wave energy. This review will first describe the dynamic aspects of auroral current structures with emphasis on consequences for models of microscopic turbulence. In the second part of the paper a number of models of microscopic turbulence will be introduced into a large-scale model of Alfvén wave propagation to determine the effect of various models on the overall structure of auroral currents. In particular, we will compare the effect of a double layer electric field which scales with the plasma temperature and Debye length with the effect of anomalous resistivity due to electrostatic ion cyclotron turbulence in which the electric field scales with the magnetic field strength. It is found that the double layer model is less diffusive than in the resistive model leading to the possibility of narrow, intense current structures.

I. INTRODUCTION

Auroral arcs and the auroral current structures which produce them occur in a variety of scale sizes and time scales. While electrostatic models of auroral electrodynamics (Lyons et al., 1979; Fridman and Lemaire, 1980; Chiu and Cornwall, 1980) have had success at describing the overall current-voltage relationship of the auroral zone and in defining the scale size of the inverted-V precipitation signature, they are not well suited to describing the dynamics of small-scale auroral arcs, multiple auroral arcs, and time-dependent auroral structures. In this realm a fluid picture of auroral electrodynamics has advantages and can describe a number of auroral processes (Sato, 1978; Goertz and Boswell, 1979; Miura and Sato, 1980; Lysak and Dum, 1983; Lysak, 1985, 1986). The difficulty with the fluid models is that the kinetic processes which play an important part in defining the auroral potential drop must be described by means of assumed transport coefficients which should be determined by a consideration of the microscopic plasma processes.

The formation of parallel potential drops in laboratory and computer simulated plasmas has been covered in many of the reviews in this workshop. The problem with applying most of these results to the auroral zone is the high sensitivity of the results to the initial and boundary conditions which are imposed. In the auroral plasma, there are no grids to be set to a certain voltage and, perhaps more fundamentally, the scale of the system is vastly larger than the sizes of a thousand Debye lengths or so which are typical in laboratory and computer studies. Therefore a description of the auroral potential drop should consider the large-scale dynamics of the auroral zone as well as the microscopic processes which can directly produce parallel electric fields.

The remainder of this review will consist of two major sections. In the first, we will consider some of the time-dependent aspects of auroral current structures and the implications these structures have for models of microscopic plasma turbulence. In particular, we will argue that auroral currents are closely associated with Alfvén wave

signatures that tend to define the current which flows along auroral field lines and that include a transient parallel electric field which can set up the particle distributions necessary to support double layer structures. In the second part of the review, we will discuss some numerical experiments in which the form of the parallel electric field is changed. We will consider two extreme cases. In the first, we assume a double layer model in which a potential drop that scales with the electron temperature is distributed over distances which scale with the Debye length when the current exceeds a threshold. We will compare this model with a model of nonlinear resistivity due to electrostatic ion cyclotron turbulence in which the effective resistivity increases with the current over a threshold. These models produce rather different overall current structures, since in the resistive model the current diffuses across the magnetic field producing broader structures, while in the double layer model narrow current structures can persist.

II. A BRIEF REVIEW OF AURORAL ELECTRODYNAMICS

The Earth's auroral zone is a region in which the ionosphere and the outer magnetosphere are coupled by means of magnetic field-aligned currents which flow between the two regions. These currents must close across field lines in the ionosphere and also somewhere in the outer magnetosphere. Ionospheric current closure is described by the current continuity equation, which is generally integrated along the field line over the thin layer (about 50 km) in which the ionospheric currents flow. To simplify the description, we will consider a two-dimensional geometry in which variations in longitude are ignored. This assumption is well justified on the dawn and dusk flanks of the magnetosphere, although it should be modified to take into account the more complicated current structures at noon and midnight. With these approximations ionospheric current continuity can be expressed as follows:

$$j_z = \frac{\partial I_x}{\partial x} = \frac{\partial}{\partial x} [\Sigma_p E_x] \quad , \quad (1)$$

where Σ_p is the height integrated Pedersen conductivity and the geometry is defined in Figure 1. Note that here a positive current is parallel to the magnetic field line, i.e., downward in the northern hemisphere.

In the steady state and in the absence of parallel electric fields, the north-south electric field E_x simply maps along the field line, which, in the dipolar coordinates of Figure 1, means that it stays constant. (More details on the dipolar coordinate system can be found in Lysak, 1985.) However, if we assume that a linear relationship exists between the parallel current and the parallel potential drop:

$$j_z = -K(\Phi_i - \Phi_e) \quad , \quad (2)$$

where Φ_i and Φ_e represent the potential in the ionosphere and in the equatorial plane, respectively, the perpendicular field must change along the field line so that the curl of the total electric field vanishes. In this case, we can combine equations (1) and (2) to relate the potential in the ionosphere to the equatorial potential:

$$\left[1 - \frac{\Sigma_p}{K} \frac{\partial^2}{\partial x^2} \right] \Phi_i = \Phi_e \quad . \quad (3)$$

This relationship indicates that large-scale potential structures in the equatorial plane, with sizes large compared to $L = \sqrt{\Sigma_p/K}$, will pass unattenuated to the ionosphere with no potential drop along the field line. On the other hand, equatorial structures with sizes less than L will not be mapped to the ionosphere, and the resulting difference will

appear as a parallel potential drop. For auroral zone parameters, this scale length L is about 100 km. This scale size is appropriate for the largest scale auroral structures, but is large compared to the sizes of individual auroral arcs which have a scale of about 1 km.

Consequences of this type of model in the steady state have been considered by Lyons et al. (1979), Chiu and Cornwall (1980), and others. Two critical assumptions are made in these models. First, it is assumed that a linear current-voltage relationship as in equation (2) is present. These authors associate such a relationship with plasma sheet particle motion in the dipolar magnetic field, as was shown by Fridman and Lemaire (1980). As we shall see below, such an approximate linear relationship is not restricted to these adiabatic models. A second assumption is that the driving force in the outer magnetosphere is characterized by a fixed potential as a function of position represented by the right-hand side of equation (3). Such a potential could be related to the $E \times B$ motion of the equatorial plasma, in which case treating it as constant implies that the equatorial convection is not affected by conditions on the field line which connects it to the ionosphere.

On the other hand, it has been known for some time that the ionosphere exerts a frictional influence on magnetospheric convection due to the dissipation caused by the finite Pedersen conductivity (e.g., Vasyliunas, 1970; Sonnerup, 1980). Information on ionospheric conditions is transmitted to the equatorial region by means of shear mode Alfvén waves which can propagate along the field line between the two regions, which have a travel time from the ionosphere to the equator of about 30 s in the auroral zone, as is evidenced by the existence of Pi2 pulsations with periods of about 2 min (Southwood and Hughes, 1983), which would correspond to the travel time from one ionosphere to the conjugate ionosphere and back.

The presence of Alfvén waves on auroral field lines should cause one to rethink the steady state model presented above. For one thing, the steady state model assumes that currents perpendicular to the magnetic field only exist at the ionosphere and in the equatorial plane, while Alfvén waves carry with them a polarization current which depends on the rate of change of the perpendicular electric field. In a static structure, these currents will vanish, but the possibility exists that a standing wave structure could be set up in which the polarization currents could persist. Such a situation is shown in Figure 2, which shows results from a time-dependent, two-dimensional MHD model of auroral currents (Lysak and Dum, 1983; Lysak, 1985). The contours in this figure represent flow lines of the current for a case in which a potential structure is propagated across the field line. Alternatively, this figure could be viewed as the current pattern produced by a potential structure in the presence of a north-south component of plasma convection in the auroral zone. As can be seen, the multiple reflections of the Alfvén wave pulses give rise to wave structure in which interference occurs between up- and downgoing waves. This wave interference decouples the field-aligned currents which connect to the ionosphere from those which flow up to the equatorial plane. In a structure such as this, which may be typical of multiple auroral arc structures, the steady state model is clearly inappropriate.

This structure can be described by a generalization of the model given above by replacing the assumption that a fixed equatorial potential structure is present by a more general assumption that a relation exists between the electric field and the perpendicular currents. For the case of polarization currents, this relation involves the so-called Alfvén conductance (Mallinckrodt and Carlson, 1978), $\Sigma_A = c^2/4\pi V_A$, where V_A is the Alfvén speed. If it is assumed that the ionospheric currents close via these polarization currents, a relation with the form of equation (3) results but with the scale length becoming:

$$L = \left[\frac{\Sigma_p \Sigma_A}{K (\Sigma_p + \Sigma_A)} \right]^{1/2} \cdot \quad (4)$$

The Alfvén conductance Σ_A is plotted along an auroral field line in Figure 3, where it can be seen that its value over the field line is generally less than the Pedersen conductivity, which is typically over 1 mho. For the Case $\Sigma_A \ll \Sigma_P$, equation (4) shows that the scale length depends on the Alfvén conductance rather than the Pedersen conductivity, leading to smaller scales than those predicted by equation (2). Thus, the 1-km scale size of discrete auroral arcs may in fact be a result of current patterns such as those shown in Figure 2.

Another process which violates the steady state assumption is the enhancement of the ionospheric conductivity due to the enhanced energetic electron precipitation produced by the parallel electric field. This can give rise to a feedback instability (Sato, 1978; Rothwell et al., 1984; Lysak, 1986) in which traveling enhancements of the conductivity and the field-aligned current occur (Fig. 4). Numerical modeling of this instability (Lysak, 1986) shows periods of about 1 s which appear to be due to Alfvén wave reflections at altitudes of $2 R_E$ or less, so these currents also close well before they reach the equatorial region. The structures shown in Figure 4 have scale sizes of about 10 km, approaching the size of the discrete aurora.

The discussion above indicates that while the steady state model can describe the large-scale properties of the aurora, time-dependent effects may be important at creating short-scale current structures on auroral field lines. Parallel electric fields thus form in a current environment which can fluctuate on time scales as quickly as 1 s. On these time scales, Alfvén waves carry changes in the field-aligned currents. Parallel electric fields form as a result (Goertz and Boswell, 1979) of the current required to flow because of the magnetic perturbation associated with the Alfvén wave. Plasma turbulence will form when the current exceeds the threshold for instabilities. The effect of this turbulence will be examined in the following section.

III. MACROSCOPIC EFFECTS OF PLASMA TURBULENCE

If plasma turbulence does develop, it can affect the development of the current structure which produced it. Lysak and Carlson (1981) showed that the introduction of parallel resistivity modified the Alfvén wave dispersion relation, producing a reflection and dissipation of the wave which reduces the current. From the point of view of the MHD equations, this is the result of the well-known magnetic diffusion equation in the presence of resistivity. Plasma turbulence in a strong magnetic field will most likely give rise to a non-isotropic conductivity. In the case of double layer formation of electrostatic ion cyclotron turbulence, the dominant effect is that of parallel resistivity (Lysak and Dum, 1983). It can be shown that this term gives rise to diffusion across the magnetic field:

$$\frac{\partial B_y}{\partial x} = \frac{\partial}{\partial x} \left[\eta_{\parallel} \frac{\partial B_y}{\partial x} \right] , \quad (5)$$

in the geometry of Figure 1 with gradients in y ignored. Thus, the presence of plasma turbulence will in general lead to a broadening of current structures and the reduction in the current strength.

In this section, we will compare three models of parallel electric fields caused by current-driven turbulence. In order to incorporate these effects into a MHD model, a simple relationship between the fluid properties of the plasma, such as density, drift velocity and temperature, and the parallel electric field, must be introduced. Clearly, a satisfactory model of this type has not yet been found and, indeed, it is likely that the complexities of plasma turbulence cannot be so easily parameterized. Nevertheless, some simple models of this type can be considered and will serve to indicate some of the relevant effects.

The first model we will consider will be based on simulations of current driven double layers (e.g., Sato and Okuda, 1981; Kindel et al., 1981; Barnes et al., 1985). When the drift velocity in these models is about half the electron thermal speed, double layers with amplitude $e\Phi/T_e \approx 1$ are produced and, in long enough systems, will recur at intervals of the order of 1000 Debye lengths, where a Debye length is the order of a few meters in the auroral plasma. Since the MHD model has a grid size along the magnetic field of about 500 km, it is appropriate to consider the average electric field, which for the above numbers leads to:

$$E_z = 0.001 [4\pi n T_e]^{1/2} \quad (6)$$

Although the drifts in excess of the threshold cause these double layers to grow and decay more quickly (Barnes et al., 1985), the average electric field over the time step of the MHD model (about 0.01 s) may remain roughly constant. To avoid a discontinuity in the electric field, the parallel field is increased linearly [using the linear resistivity given by equation (9) below] until the double layer electric field given above is reached. It should be noted that double layer electric fields are not present when the plasma frequency exceeds the electron cyclotron frequency (Barnes et al., 1985). This effect has not been explicitly included in the model; however, in the region in which the critical current is the lowest, the plasma frequency remains below the cyclotron frequency.

As an alternate to the double layer model, we consider a model for electrostatic ion cyclotron (EIC) turbulence due to resonance broadening (Dum and Dupree, 1970; Lysak and Dum, 1983). In this model, a resistive potential drop is introduced whenever the current exceeds the threshold for the EIC instability, i.e., about 0.3 of the electron thermal speed for $T_e = T_i$. The amplitude of the fluctuating electric field, and thus the effective resistivity, increases quadratically as the current increases. Thus, the electric field becomes:

$$E_z = \frac{m\nu^*}{ne^2} (j_z - j_{crit}) \quad (7)$$

where the effective collision frequency is:

$$\nu^* = 0.4 \Omega_i \left[1 + 0.1 \left(\frac{j_z - j_{crit}}{j_{crit}} \right)^2 \right] \quad (8)$$

Note that in this case the parallel electric field will scale with the strength of the background magnetic field through the ion gyrofrequency $\Omega_i = eB/m_i c$, in contrast to the double layer model described by equation (6).

These two models have very differing behavior in that the double layer model is electric field-saturated in the sense that once the critical current is reached, the parallel electric field does not increase further. The nonlinear resistive model described by equations (7) and (8) is in a sense current-saturated since the electric field rises very rapidly after the critical current is reached. This enhances the diffusion of the current and reduces it to a lower level. The third model that will be considered will be one in which an effective collision frequency is assumed as in equation (7) but the collision frequency is independent of the current once the threshold is reached. Thus, equation (8) is replaced by:

$$\nu^* = 0.4 \Omega_i \quad (9)$$

when the drift velocity exceeds 0.3 of the electron thermal speed. This model will be referred to as the linear resistivity model.

In order to assess the macroscopic consequences of these models, a series of runs were done with the MHD model described earlier. In these runs, a current loop of a fixed magnitude and width is introduced on the field line, propagates toward the ionosphere, and enters a region of parallel electric field described by one of the three models. The ionospheric conductivity is taken to be fixed at 1 mho, and the density profile is of the form:

$$n(r) = 10^5 e^{-(r-r_0)/h} + 5 (r - 1)^{1.5} , \quad (10)$$

where n is measured in cm^{-3} , r is in R_E , the base altitude for the ionosphere is $r_0 = 1.05 R_E$, and the scale height $h = 0.1 R_E$. The electron temperature is 1 eV and the upper boundary condition is taken to absorb Alfvén waves which are incident upon it after being reflected from lower altitudes (Lysak, 1985). As the runs proceed, the maximum potential drop and the field-aligned current at the ionosphere are monitored, as the system approaches a steady state. Since the ionosphere is a very good conductor, the current of a reflected Alfvén wave is in the same direction as that of the incident wave (Mallinckrodt and Carlson, 1978); thus, the final value of the current will be twice the injected current in the limit of infinite ionospheric conductivity ($\Sigma_P \gg \Sigma_A$) and no parallel electric field. Such a case is shown in Figure 5 in which the injected current was $20 \mu\text{A}/\text{m}^2$ and the final current of $36 \mu\text{A}/\text{m}^2$ is nearly double this value. Because of the diffusion associated with the parallel electric field, the current reaching the ionosphere is reduced when a parallel electric field is present. This effect is shown for the double layer model and the nonlinear resistivity model in Figures 6 and 7, respectively. In these figures the injected current was $20 \mu\text{A}/\text{m}^2$. It can be seen that the double layer model is much less diffusive than the resistive model, with the final currents being $30 \mu\text{A}/\text{m}^2$ and $6 \mu\text{A}/\text{m}^2$ for the two runs.

The final current-voltage characteristics for a series of runs are shown in Figure 8. First of all, note that each of the models produces potentials in the kilovolt range for currents of a few microamps per square meter. This is significant since the parameters of the parallel electric field model were determined purely from the local properties of the auroral plasma without any requirement that the global current-voltage relation come out right. Therefore, none of the models can be ruled out on this basis.

Turning to differences in the models, we see that the double layer model exhibits the voltage-saturation effect referred to earlier. As the current increases, more of the field line can support the formation of double layers, leading to an increased total potential drop. Since it is assumed that the parallel electric field does not increase further as the current increases, the addition of more current does not further increase the total potential drop.

The linear resistivity model produces a linear current-voltage characteristic. At first glance this may appear obvious, but actually the situation is complicated by the scaling of the fields and currents along the field line. It was shown by Lysak and Dum (1983), however, that these factors cancel when the resistivity scales with the magnetic field strength, preserving the linear relationship between the total potential and the field-aligned current at the ionosphere. The approximate linear relationship has been invoked by Lyons (1980) to support the nonlocal current-voltage relationship based on adiabatic particle motions (e.g., Fridman and Lemaire, 1980). However, the present argument shows that this interpretation is not unique.

The current limiting effect of the nonlinear resistivity model is apparent from Figure 8. Here an attempt to increase the current simply causes an enhancement in the diffusion, leading to large potentials and a broader current structure as is seen in Figures 9 and 10, which compare the field and current profiles for the double layer and non-linear resistivity models. Here the enhanced diffusion due to the nonlinear resistivity is evident.

Figure 11 shows the effective diffusion in the entire set of runs by plotting the ratio between final and input currents against the input current. As discussed above, the maximum value of this ratio is 2 for the case of infinite Pedersen conductivity. The open squares represent runs with no parallel electric field and a Pedersen conductivity of 1 mho. The small reduction from 2 in these cases represents the effect of ionospheric dissipation. Note that the linear and nonlinear resistive models have comparable diffusion for small currents where the nonlinear part of the resistivity is not important; but, at larger currents, the nonlinear model is more diffusive. The double layer model is comparable to the other models at low currents, but an increase in the current decreases the effective diffusion since the potential drop does not increase for increasing current.

In summary, the three models for a local current voltage relation produce results consistent with the observed global relationship. Thus, this type of model cannot be distinguished from the kinetic models of parallel potential drop on this basis. The double layer model allows for very strong currents to flow in a narrow channel since the potential drop and thus the effective diffusion do not increase much as the current increases. The nonlinear resistive model has the opposite effect in that the strong increase in the potential drop for an increase in the current causes an enhanced diffusion which broadens the current channel, in effect causing the current to flow around the region of parallel electric field.

IV. SUMMARY AND CONCLUSIONS

The simplified models of parallel electric fields presented here have provided some insight into the development of the auroral potential drop, but are clearly limited in their applicability to the auroral plasma. Auroral conditions can be quite varied, and the presence of turbulence along the field line can result in the heating of the plasma as well as a decrease in the plasma density as transversely heated ions are expelled from the acceleration region. Therefore, there is more to auroral dynamics than can be found in the simple cold plasma model used here.

Density decreases in the auroral zone serve to decrease the critical current necessary for the generation of microscopic turbulence, and therefore will increase the total potential drop for a given level of current. Numerical results indicate that this result is more important in the double layer model because of the "switch-on" nature of the double layer electric field. Since the double layer electric field scales with the plasma pressure, the potential drop is localized at the lowest altitudes at which the critical current is exceeded. This is in contrast with the resistive electric field which depends on the excess current over the critical current, and thus maximizes at the point where the critical current is lowest. A set of runs in which a current of $10 \mu\text{A}/\text{m}^2$ is injected showed that the potential drop increased by 25 percent in the double layer model when the ionospheric scale height [see equation (10)] is reduced to $0.05 R_E$ from the value of $0.1 R_E$ used in the other runs, while in the nonlinear resistivity model the increase was only 18 percent. Thus, the effect of a density cavity would be to produce an increase in the potential drop, especially in the double layer model.

The temperature of the topside ionosphere can also vary under auroral conditions, and may be expected to increase as the result of microscopic turbulence. Increases in the temperature will tend to decrease the extent of the turbulent region since the critical current scales as the electron thermal speed. Thus, potential drops due to nonlinear resistivity would be expected to decrease. A similar result is true in the double layer model; however, this effect is counteracted by the increase of the average electric field due to double layers since this field scales with the square root of the temperature. Runs at $10 \mu\text{A}/\text{m}^2$ indicate that the potential drop in the nonlinear resistivity model decreased by 35 percent when the temperature was raised by a factor of 10, while in the double layer model the potential increased by 12 percent. Thus, the increase of temperature favors the double layer model, at least until the point at which the current becomes sub-critical.

In the actual auroral zone, these two effects will be necessarily connected. The transverse heating of ions observed in the auroral zone can create density cavities since the heated ions are subject to the magnetic mirror force that expels them from the low-altitude auroral zone. One can imagine a scenario in which the increase of the current magnitude excites turbulence, leading to the heating of ions and the creation of the density cavity. This hot, low density plasma would lead to conditions under which the formation of double layers could further accelerate electrons into the atmosphere and ions out of the atmosphere. This would result in the density cavity progressively extending to lower and lower altitudes, with a corresponding increase in the total potential drop along the field line. While the existing numerical model is too crude to account for all these effects, this scenario seems plausible based on the results above. A more complete model including the effects of the thermal evolution of the plasma will be the subject of future work.

In conclusion, this work has shown first of all that models of the auroral potential drop based on microscopic turbulence, whether due to double layers or a nonlinear resistivity, can account for the correct magnitude of the auroral potential drop for typical auroral currents. The two models differ in that the nonlinear resistivity model limits the current density by spreading the current over a broader area. In contrast, the double layer model proposed above has a limit to its total potential drop and can sustain currents with a high density. At such high current densities, however, this model will most likely be too simplified, since plasma heating and the formation of a density cavity, effects not included in the cold plasma model presented here, will likely change the nature of the current-voltage relation.

The oversimplified models presented here represent an attempt to incorporate kinetic effects of the plasma into a fluid model. In order to model the global structure of the auroral zone, some such approximation must be made since particle-in-cell or Vlasov models of any large volume of the auroral zone are technically not feasible with present or anticipated computer resources. The question of a satisfactory parameterization of the kinetic effects for use in a fluid model remains an open question, which can only be answered by a combination of fluid modeling and kinetic modeling, as well as analytic theory of the auroral current region.

Acknowledgments. The authors would like to thank W. Lotko and D. S. Evans for useful discussions on this work. This work was supported in part by NSF grants ATM-8451168 and ATM-8508949 and NASA grant NAGW-809. Computing costs were supported by the University of Minnesota Supercomputer Institute.

REFERENCES

- Barnes, C., M. K. Hudson, and W. Lotko, *Phys. Fluids*, 28, 1055 (1985).
- Chiu, Y. T., and J. M. Cornwall, *J. Geophys. Res.*, 85, 543 (1980).
- Dum, C. T., and T. H. Dupree, *Phys. Fluids*, 13, 2064 (1970).
- Fridman, M., and J. Lemaire, *J. Geophys. Res.*, 85, 664 (1980).
- Goertz, C. K., and R. W. Boswell, *J. Geophys. Res.*, 84, 7239 (1979).
- Kindel, J. M., C. Barnes, and D. W. Forslund, in *Physics of Auroral Arc Formation*, American Geophysical Union *Geophysical Monograph* 25, edited by S.-I. Akasofu and J. R. Kan, p. 296, 1981.
- Lyons, L. R., *J. Geophys. Res.*, 85, 17 (1980).
- Lyons, L. R., D. S. Evans, and R. Lundin, *J. Geophys. Res.*, 84, 457 (1979).
- Lysak, R. L., and C. W. Carlson, *Geophys. Res. Lett.*, 8, 269 (1981).
- Lysak, R. L., and C. T. Dum, *J. Geophys. Res.*, 88, 365 (1983).
- Lysak, R. L., *J. Geophys. Res.*, 90, 4178 (1985).
- Lysak, R. L., *J. Geophys. Res.*, accepted for publication, 1986.
- Mallinckrodt, A. J., and C. W. Carlson, *J. Geophys. Res.*, 83, 1426 (1978).
- Miura, A., and T. Sato, *J. Geophys. Res.*, 85, 73 (1980).
- Rothwell, P. L., M. B. Silevitch, and L. P. Block, *J. Geophys. Res.*, 89, 8941 (1984).
- Sato, T., *J. Geophys. Res.*, 83, 1042 (1978).
- Sato, T., and H. Okuda, *J. Geophys. Res.*, 86, 3357 (1981).
- Sonnerup, B.U.O., *J. Geophys. Res.*, 85, 2017 (1980).
- Southwood, D. J., and W. J. Hughes, *Space Sci. Rev.*, 35, 301 (1983).
- Vasyliunas, V. M. in *Particles and Fields in the Magnetosphere*, edited by B. McCormac, p. 29, D. Reidel, Hingham, Massachusetts, 1970.

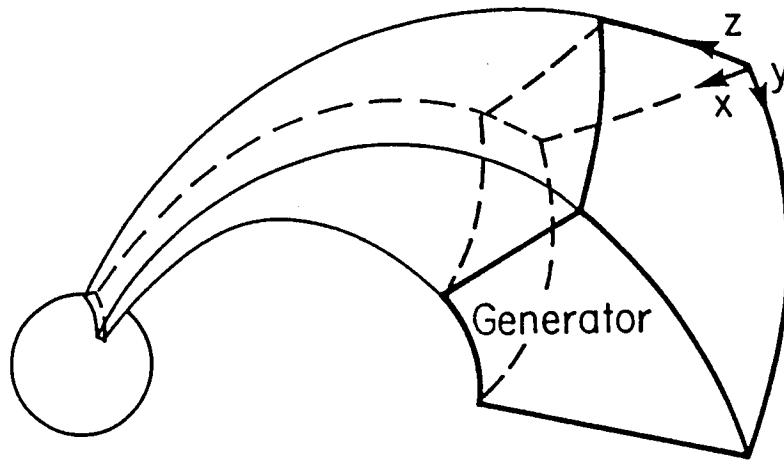


Figure 1. A sketch of the dipolar coordinate system used in this paper. Here z is the coordinate along the geomagnetic field, y is the longitude, and x is a coordinate proportional to the inverse of the L value of the field line.

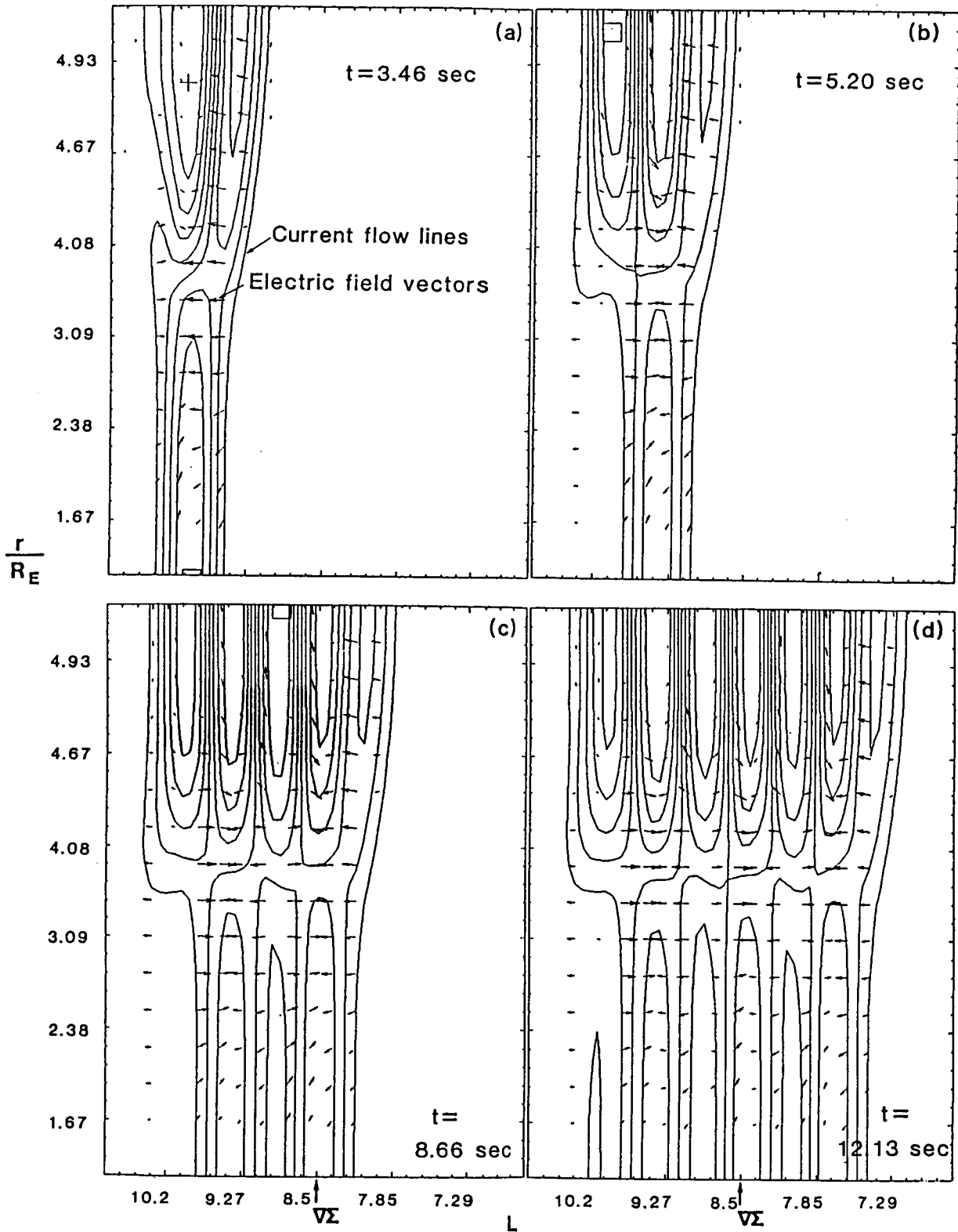


Figure 2. A set of snapshots showing the evolution of a run in which a moving voltage pulse travels across field lines (Lysak, 1985). The contour lines represent current flow lines in the xz plane of Figure 1. Note that the currents which reach the ionosphere close in the region between 3 and $4 R_E$ where up- and downgoing waves interfere.

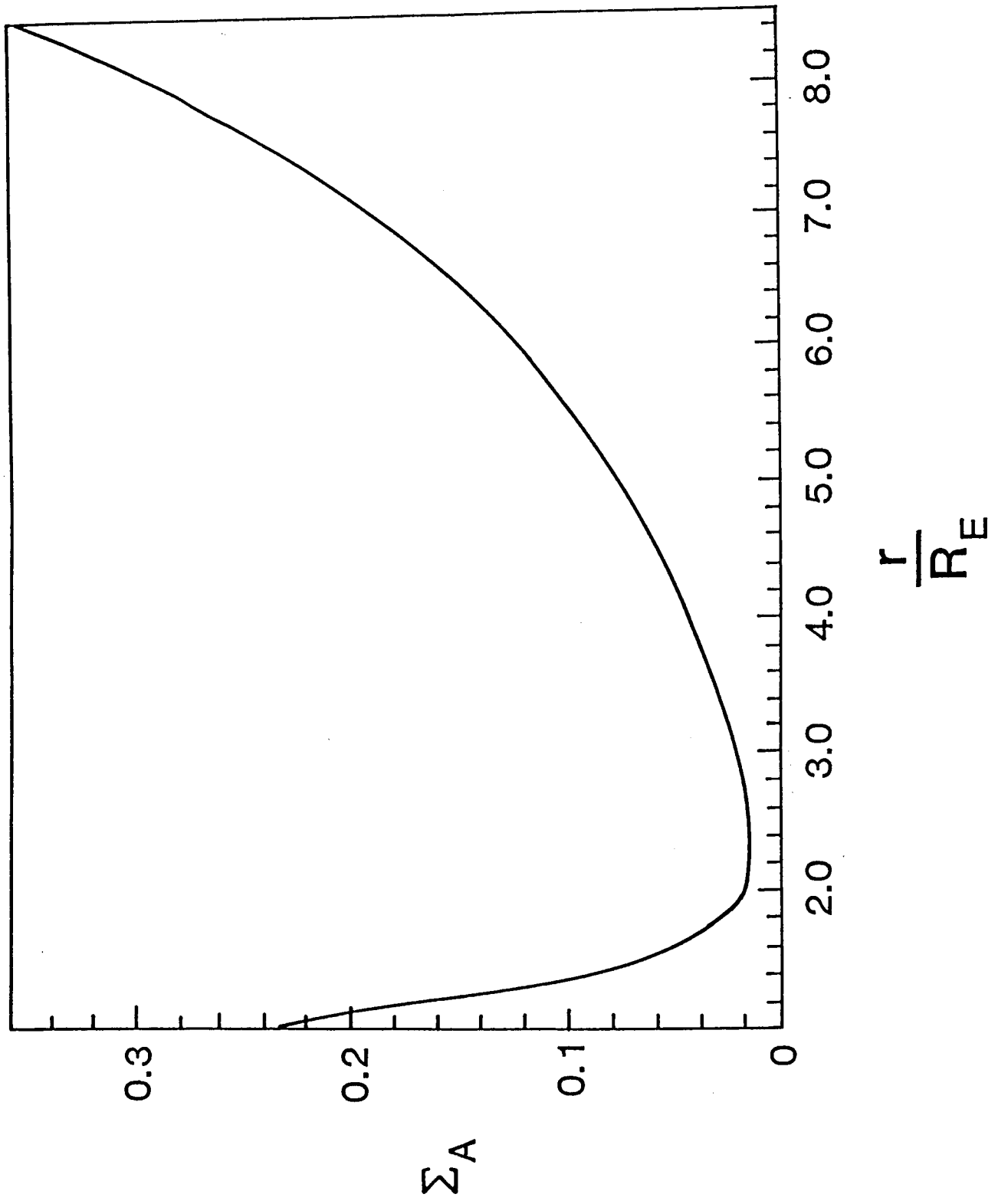


Figure 3. A sketch of the Alfvén wave admittance Σ_A (in mho) as a function of radial distance for the density profile given by equation (10).

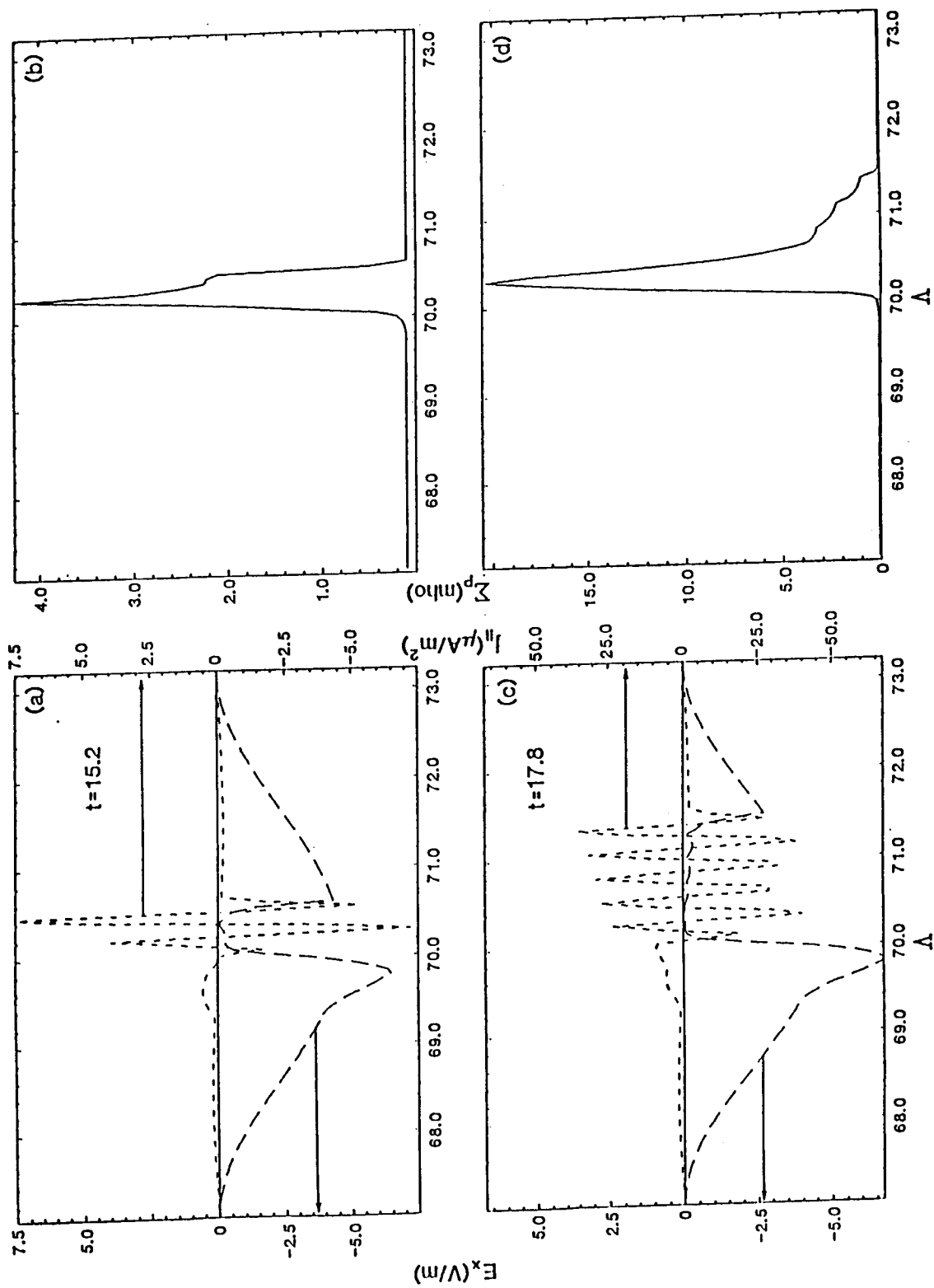


Figure 4. Ionospheric electric field, field-aligned currents, and Pedersen conductivity for a run in which the conductivity increases due to electron precipitation and a feedback instability results (Lysak, 1986). The oscillations in the current have a wavelength of about 20 km and a frequency of near 1 Hz, indicative of wave reflection from the region of minimum wave admittance.

Run number 258, Ionospheric current history

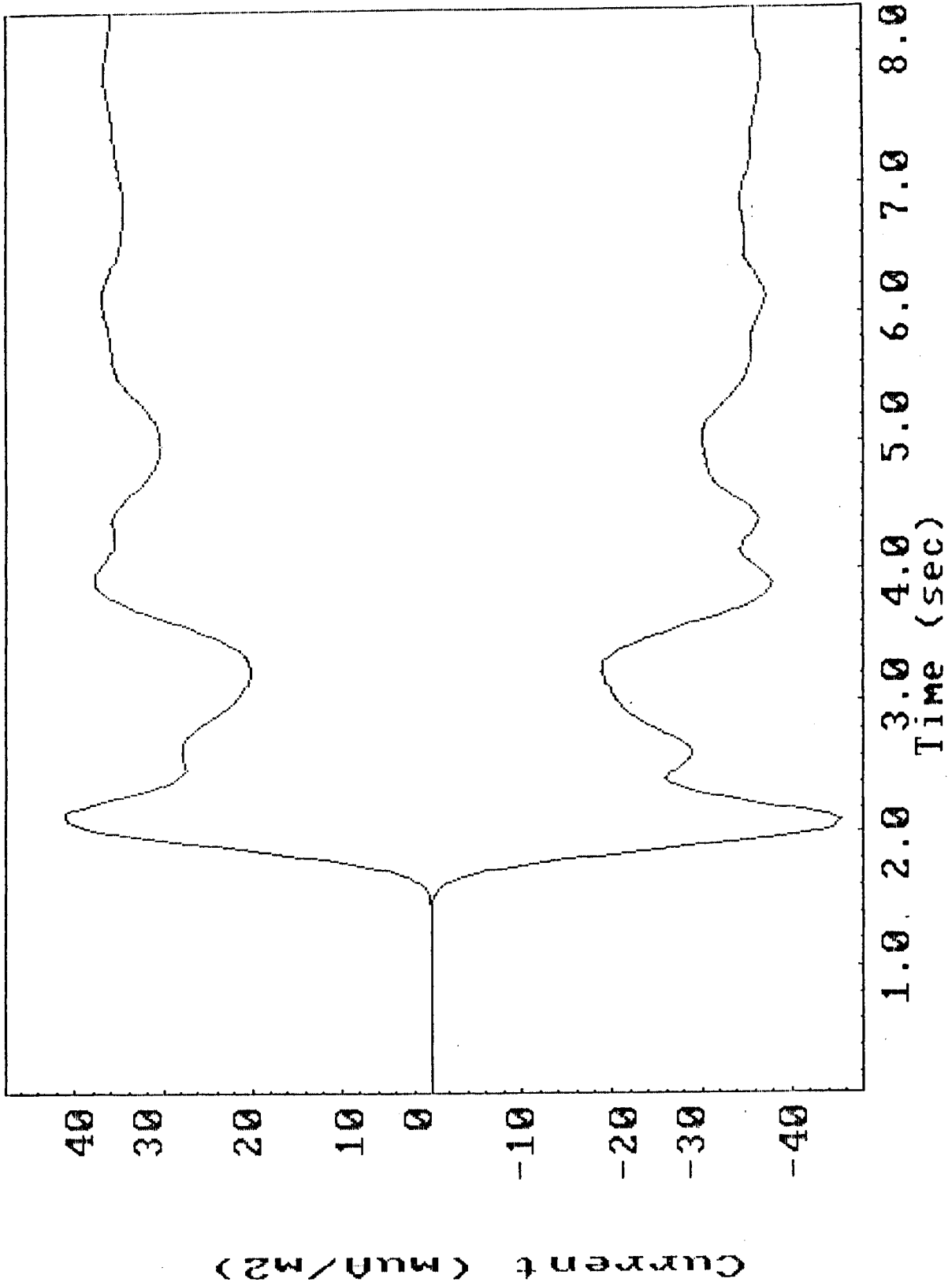


Figure 5. Maximum and minimum field-aligned currents at the ionosphere for a run with a Pedersen conductivity of 1 mho, an injected current of $20 \mu\text{A}/\text{m}^2$, and no parallel electric field. The maximum current attainable in this system is $40 \mu\text{A}/\text{m}^2$, and the final value of $36 \mu\text{A}/\text{m}^2$ is due to losses in the ionosphere.

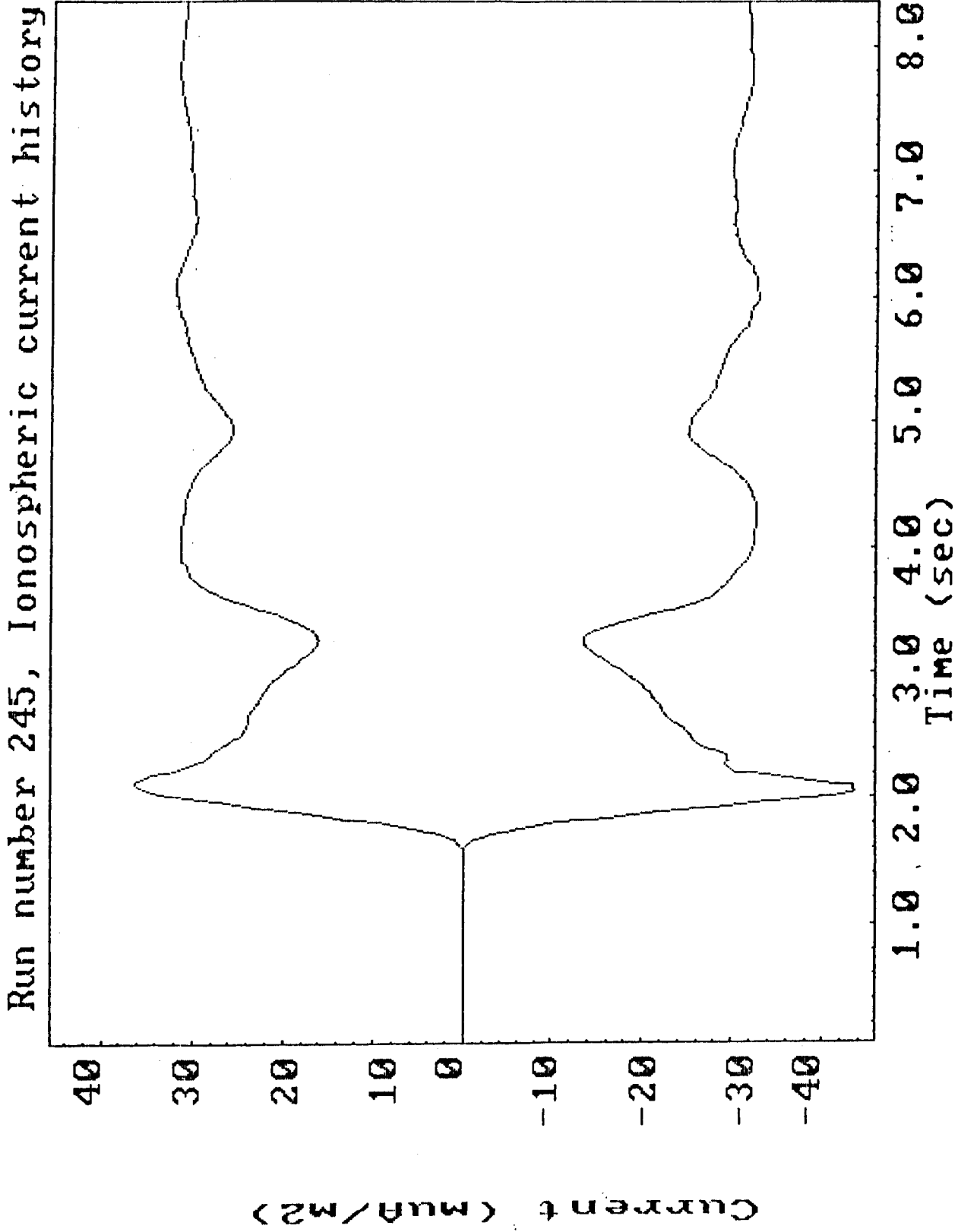


Figure 6. Similar to Figure 5 except that a double layer electric field has been included. The maximum current is reduced to $30 \mu\text{A}/\text{m}^2$ in this case.

Run number 246, Ionospheric current history

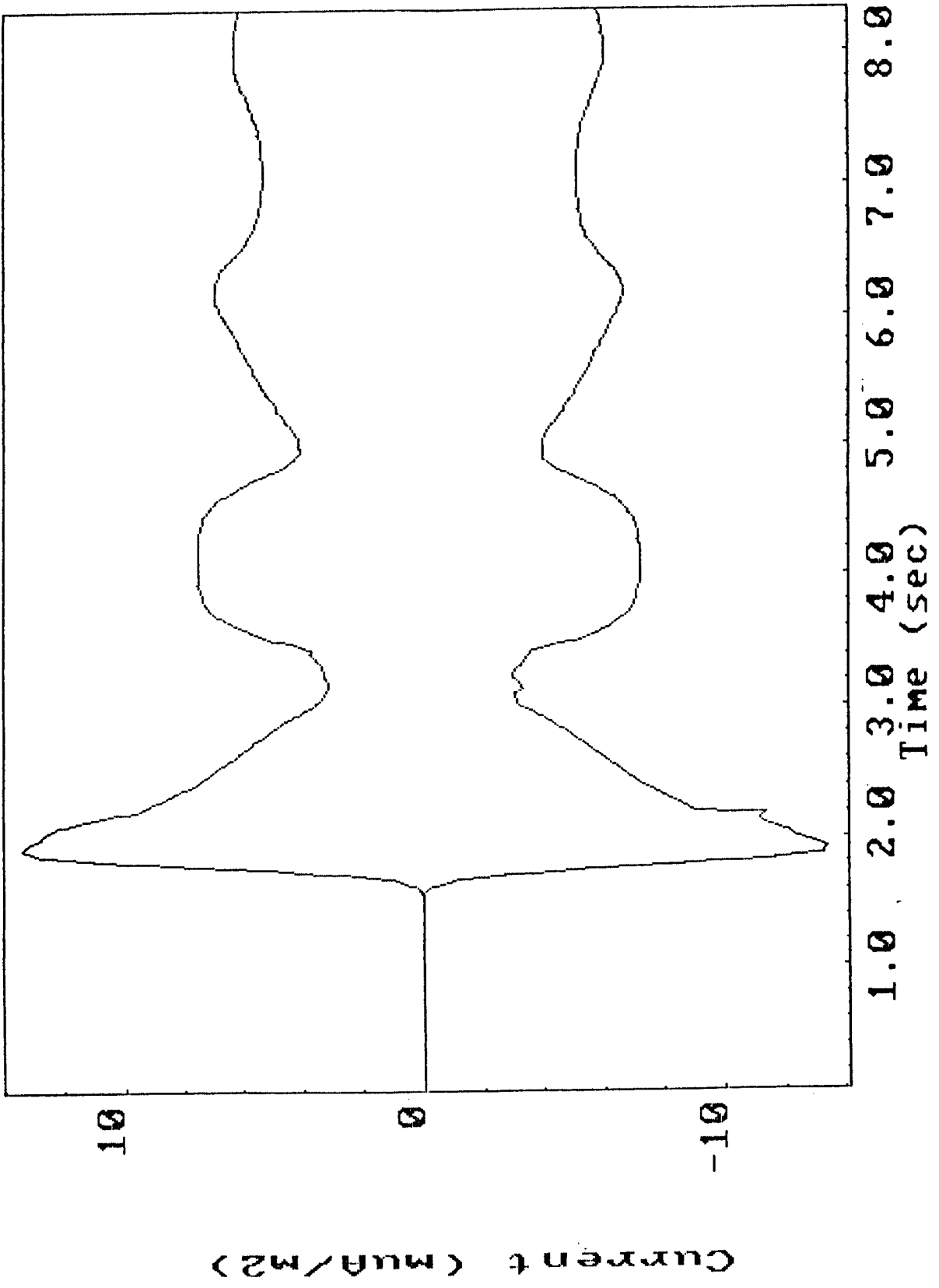


Figure 7. Similar to Figures 5 and 6 but including a nonlinear resistivity. The maximum current is drastically reduced due to the diffusion of the current structure to $6 \mu\text{A}/\text{m}^2$.

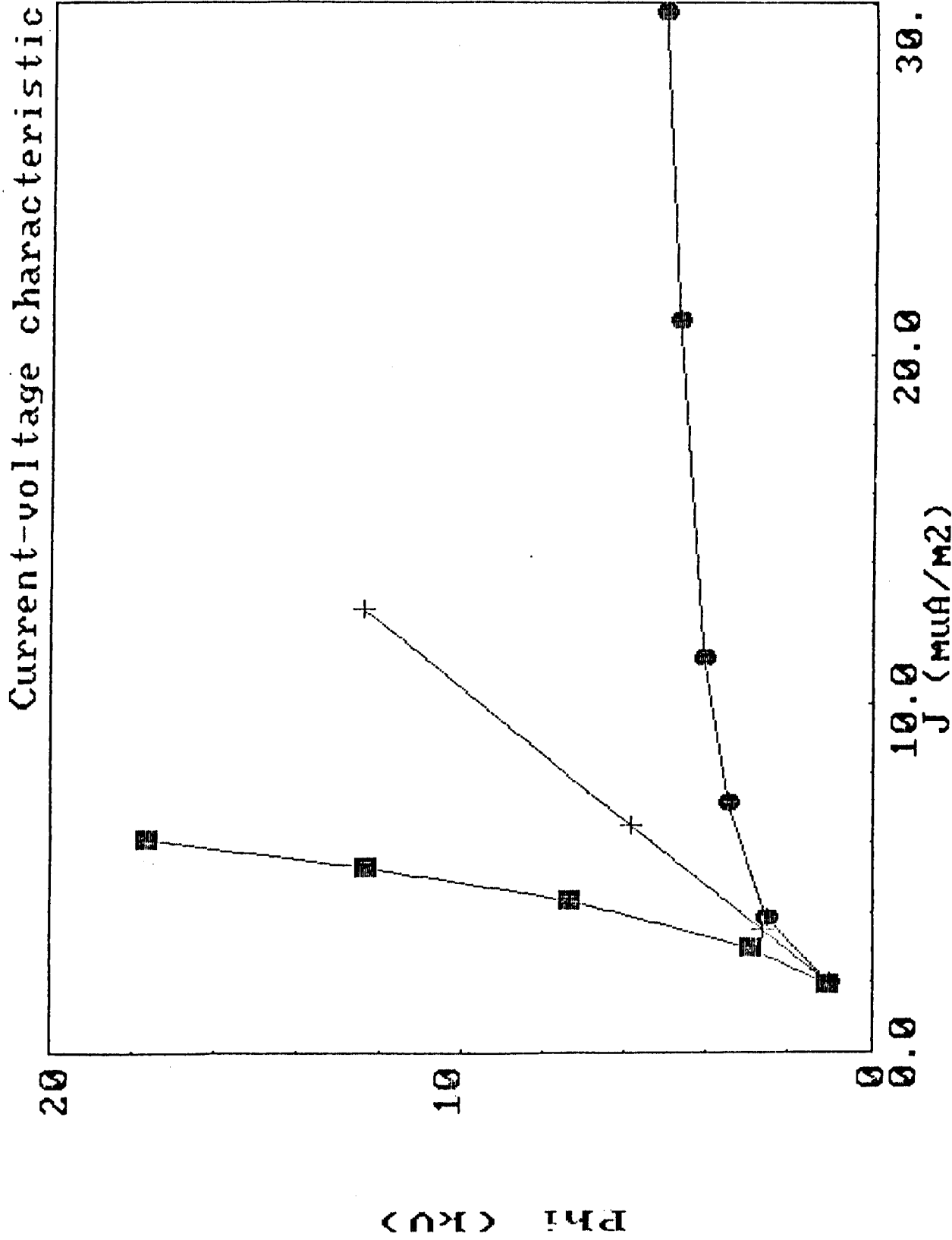


Figure 8. Current-voltage characteristics for a set of runs comparing the double layer model (dots), linear resistivity model (crosses), and the nonlinear resistivity model (squares).

Run 245, Fields, t=8.35, r=1.99

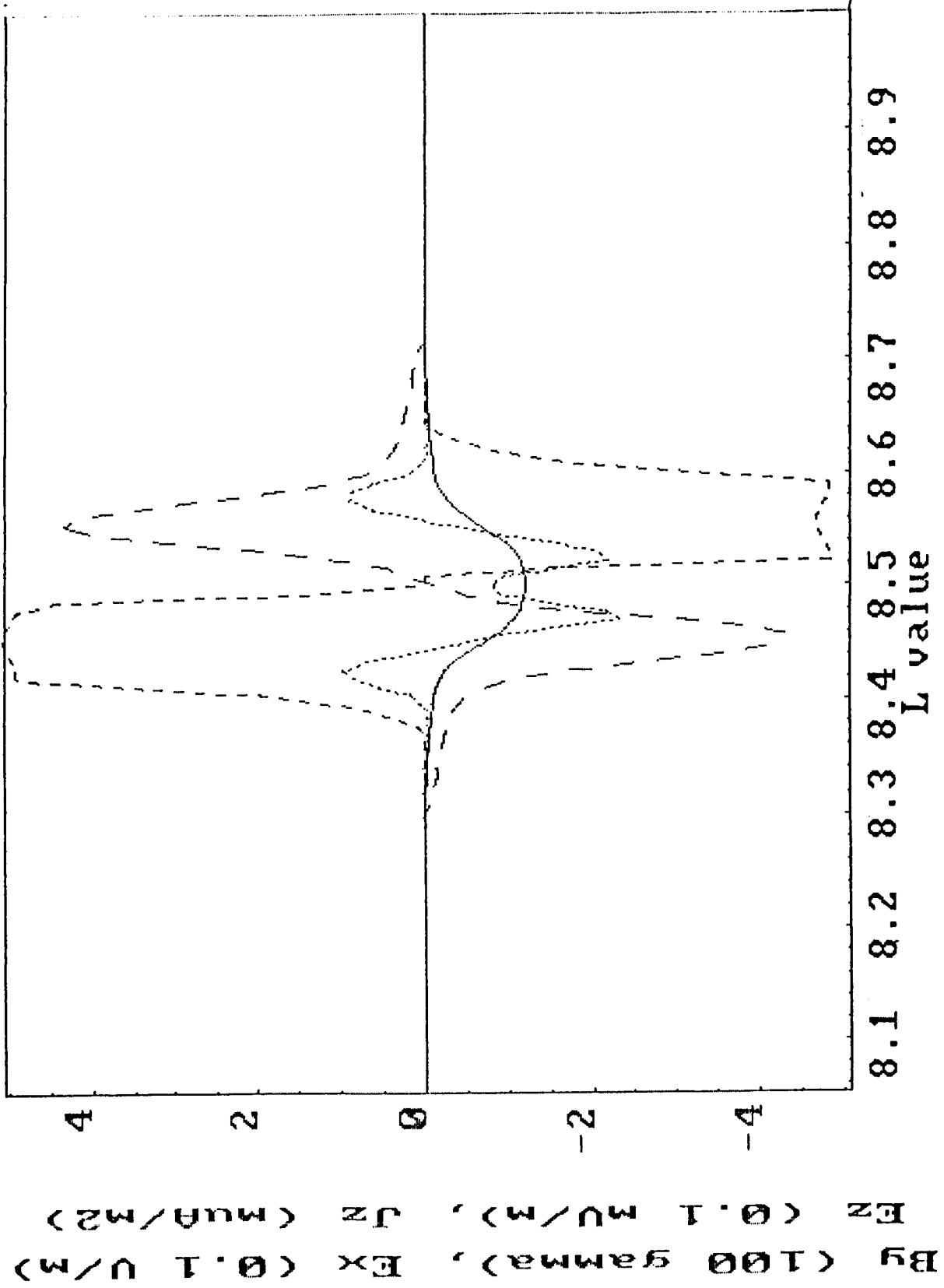


Figure 9. Field profiles at $2 R_E$ for the double layer run of Figure 6. The solid line gives the magnetic perturbation, the dotted line the perpendicular electric field, the short dashed line the parallel electric field, and the long dashed line the field-aligned current. These fields are in units of 100γ , 0.1 V/m , 0.1 mV/m , and $\mu\text{A/m}^2$, respectively.

Run 246, Fields, t=8.35, r=1.99

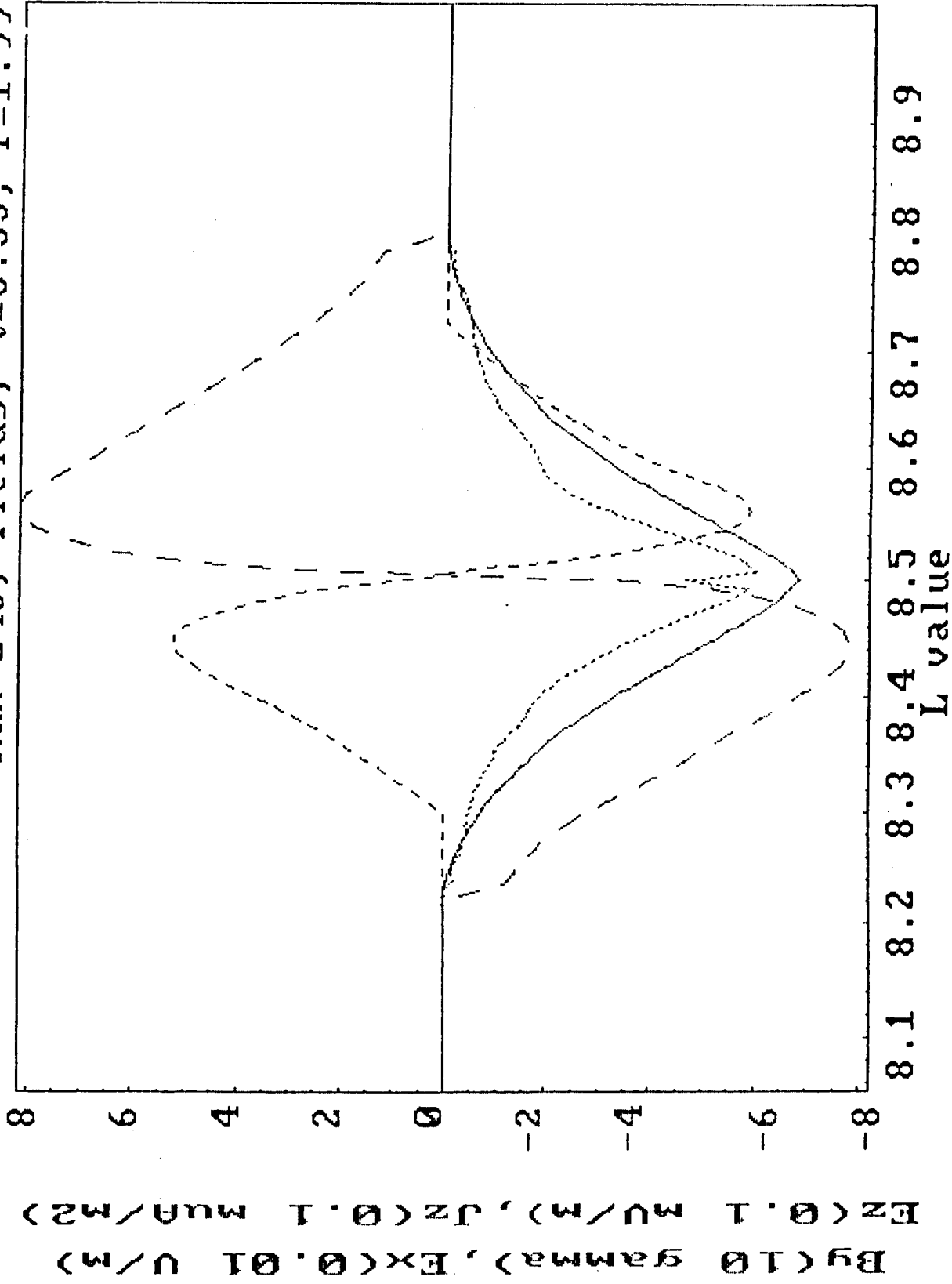


Figure 10. Same as Figure 9 but for the nonlinear resistivity run of Figure 7. The units in this case are $10^{-1} \mu A/m^2$ for B_x, E_x, E_z , and J_z , respectively. V/m , $0.1 mV/m$, and $0.1 \mu A/m^2$ for B_y, E_y, E_z , and J_y , respectively.

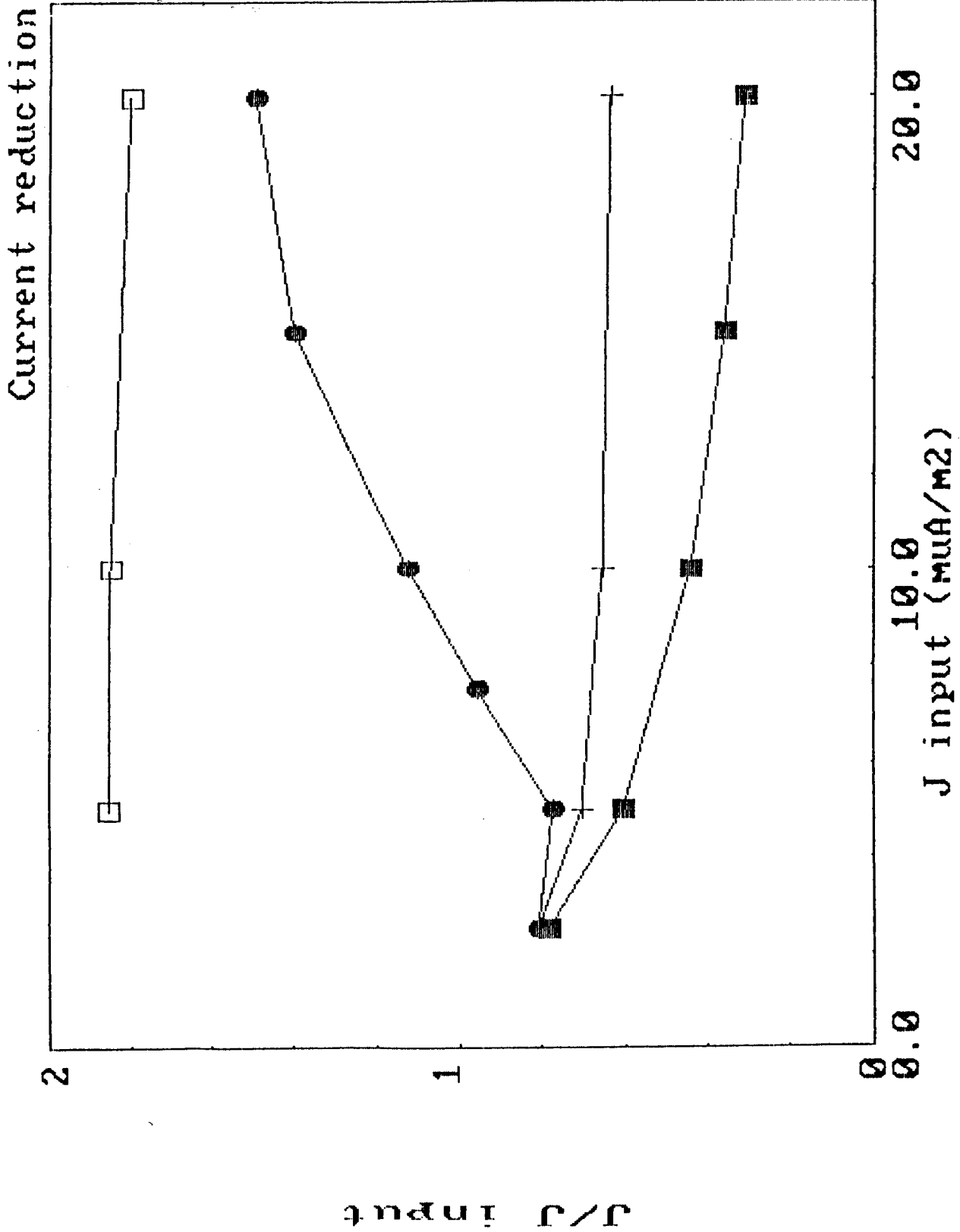


Figure 11. A comparison of the final currents to the injected currents for the runs of Figure 8, using the same symbols. In addition, runs in which no parallel electric fields were included are indicated by open squares.